samples by iterative thermal oxidation in air. AFM (atomic force microscope) measurements were carried out after every few hours of oxidation and removal of the oxide in a diluted (2%) HF solution [23]. The r.m.s. (root-mean-square) roughness versus oxidation time is shown in Fig. 4a. In the best case, the mirror roughness was reduced from 3.4nm to 1.7nm, while in the two other samples the roughness was reduced to about 2.5nm. This is consistent with the work by Lai [24] who reported that the final roughness achievable from this method is determined by its initial roughness.

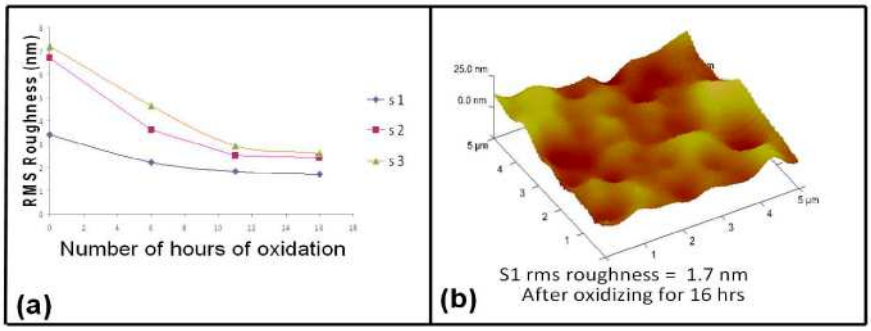

Fig. 4. (a) is a plot showing the r.m.s. roughness versus oxidization time for three different samples s1, s2 and s3. (b) shows the AFM image of the sample with the lowest r.m.s. roughness of 1.7 nm over an area of 5 x 5µm.

Electropolishing instead of KOH was used to remove the PSi because KOH is an anisotropic etchant in which the etch rate is plane dependent. For a concave mirror, the effect of any KOH exposure is immediately apparent since such a wide angular range of crystalline planes are exposed, as shown in Fig. 5a. Such "blossom" patterns resulting from KOH etching was reported previously [25], and rapidly ruins the uniform profile of any concave surface. In comparison, the PSi on the concave mirror in Fig. 5c which was removed by electropolishing has no 'blossom' patterns and the concave mirror is able to focus incoming light into a single bright spot.

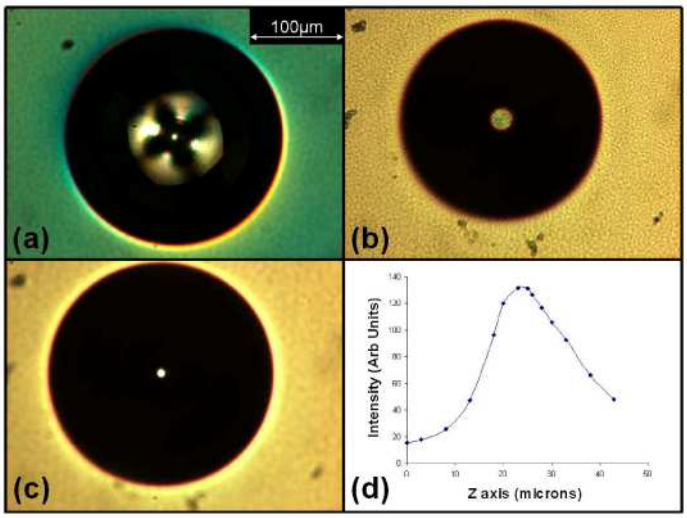

Fig. 5. (a) shows the 'blossom' pattern on a concave mirror resulting from the anisotropic KOH removal of PSi. In (b), the Psi was removed by electropolishing. (c) is an optical image of a concave mirror where the bottom of mirror is in focus. (d) is a plot of the intensity of the bright spot in the center of a concave mirror versus the microscope stage vertical position measured from the bottom of the concave mirror. The highest intensity is measured to be ~25 µm from the bottom of the mirror and this may be taken to be the focal length of the mirror.

#128374 - $15.00 USD Received 13 May 2010; revised 15 Jun 2010; accepted 15 Jun 2010; published 22 Jun 2010

In Fig. 5b, c and d, the focal length of a D = 100μm concave mirror was characterized using an optical microscope. In Fig. 5b, the microscope was positioned with the base of the mirror in focus. The sample was then moved vertically downwards until the curved region of the mirror focuses into a bright spot in Fig. 5c. Intensity measurements of the spot are shown in Fig. 5d. The focal length is taken to be where the intensity of the central spot is the highest, equal to ~25μm here. This further shows that the concave mirrors are spherical since spherical mirrors have a focal length of half their radius.

3.2 Concave PSi multilayer distributed Bragg reflectors

Distributed Bragg reflectors are multilayer structures with alternating high and low refractive indices. Each layer has an optical thickness of $\lambda/4 = nd$, where n is the refractive index, d is the thickness and λ is the reflected wavelength. Through the multiple reflections from each successive layer, together with constructive and destructive interferences, a Bragg reflector is able to reflect at particular wavelength λ from an incident light orthogonal to the surface.

PSi was demonstrated to be a good material for the fabrication of such multilayered structures [26]. The refractive index n of a single PSi layer is dependent on the porosity which is in turn dependent on the current density used during the anodisation process. The formation of PSi is self-limiting, hence, to create a PSi based Bragg reflector, one just alternates the etch current densities during anodisation to create layers with alternating high/low refractive indices as in Fig. 3a. The use of ion irradiation to slow down PSi formation was successfully used to tune the reflectivity of such Bragg reflectors [18] as well as to fabricate three dimensional Bragg reflectors [27]. Here we describe the fabrication of PSi multilayer Bragg reflectors on the concave etched surfaces, giving the ability to selectively reflect and focus particular wavelengths.

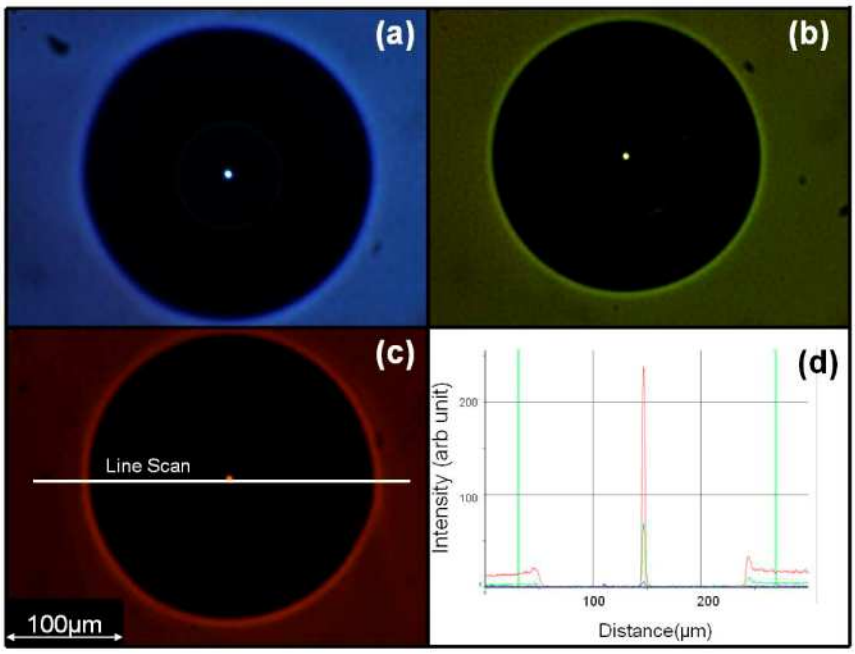

Fig. 6. (a), (b) and (c) are optical images of concave Distributed Bragg mirrors designed to focused and reflect blue, green and red respectively. These concave Bragg mirrors are illuminated with white light and they correctly select and focused their respective colors. A line scan was taken across the red concave Bragg mirror as shown in (c) and is plotted in (d). The plot correctly show that red is the dominant color focused to a point.

The concave mirrors described above were then used to form concave multilayer PSi Bragg reflectors. Three samples were etched to select and focus red, green and blue at 630nm,

#128374 - $15.00 USD Received 13 May 2010; revised 15 Jun 2010; accepted 15 Jun 2010; published 22 Jun 2010

530nm and 450nm respectively from a white incident light. They were fabricated to have 20 sets of bilayers with alternating current densities of 10mA/cm^2 and 70mA/cm^2. The anodization thickness of each layer was varied to have different optical thickness *nd* corresponding to one quarter of their respective wavelength.

Figure 6a, b and c shows the optical images of successfully fabricated concave PSi Bragg reflectors designed to reflect blue, green and red. These concave Bragg reflectors were illuminated with a parallel white light source and the concave Bragg reflectors then select the respective wavelengths and focus them into a single spot. The reflectivity of the red-reflecting concave Bragg reflectors is further characterized in Fig. 6d. With the aid of a microscope, a line scan measuring the intensity of the red, green and blue spectral components was measured across the focused point (Fig. 6c) and plotted in Fig. 6d. The line scan shows the dominant red color that this mirror was designed to reflect and focus. It also shows that the mirror focuses the incoming light down to a beam spot of approximately 1μm (FWHM from Fig. 6d). This line scan plot very appropriately shows both the focusing and wavelength selective properties of these curved PSi Bragg reflectors concurrently. This work also demonstrates the ability to form curved PSi distributed Bragg reflectors, in which each layer remains parallel to those above and below it. While these Bragg Reflectors have been demonstrated for visible wavelengths, it can easily be extended to the infra-red simply by increasing the thickness of each layer in the multilayer.

4. Conclusion

We have fabricated Si concave spherical mirrors and concave cylinders with low roughness and demonstrated the ability to do so repeatedly and controllably. The location, diameters and the height of the concave mirrors and concave cylinders may be controlled and are limited primarily by the patterning of the photoresist patterns during the UV lithography step. These concave structures have a variety of applications ranging from MEMS and optoelectronics to lab-on-chip devices. They may also be used as templates or molds to produce microlenses on polymers. By using these concave mirrors in conjunction with plane mirrors, small optical cavities can be built for single atom detection or quantum information control through cavity QED effects. In addition, using these concave mirrors as a starting material, we have also fabricated concave PSi based Bragg reflectors which are able to have wavelength selective focus. This will be useful for telecommunications or to be used as optical interconnects.

Acknowledgements

Funding support by the Singapore Ministry of Education Academic Research Fund Tier 2 under Grant No.T207B1110 is acknowledged.

#128374 - $15.00 USD Received 13 May 2010; revised 15 Jun 2010; accepted 15 Jun 2010; published 22 Jun 2010